Ecological selectivity and the evolution of mammalian substrate preference across the K–Pg boundary

Article type: Original Research

Running title: Arboreal mammals and the K–Pg extinction

Jonathan J. Hughes[1,λ,*], Jacob S. Berv[1,2,3,λ], Stephen G. B. Chester[4,5,6], Eric J. Sargis[7,8,9], Daniel J. Field[10,11*]

1. Department of Ecology & Evolutionary Biology, Cornell University, Ithaca, NY, USA
2. Department of Ecology & Evolutionary Biology, University of Michigan, Ann Arbor, MI, USA
3. University of Michigan Museum of Paleontology, University of Michigan, Ann Arbor, MI, USA
4. Department of Anthropology, Brooklyn College, City University of New York, Brooklyn, NY, USA
5. Department of Anthropology, The Graduate Center, City University of New York, New York, NY, USA
6. New York Consortium in Evolutionary Primatology, New York, NY, USA
7. Department of Anthropology, Yale University, New Haven, CT, USA
8. Divisions of Vertebrate Paleontology and Vertebrate Zoology, Yale Peabody Museum of Natural History, New Haven, CT, USA
9. Yale Institute for Biospheric Studies, New Haven, CT, USA
10. Department of Earth Sciences, University of Cambridge, Cambridge, UK
11. Museum of Zoology, University of Cambridge, UK

[λ]Authors contributed equally

*Authors for correspondence: jjh359@cornell.edu; djf70@cam.ac.uk

Abstract word count: 230

Total word count: 5547

Keywords: Placentals, Marsupials, Euarchontans, Substrate use, Paleoecology, Ancestral state reconstruction

Abstract

The Cretaceous-Paleogene (K–Pg) mass extinction 66 million years ago was characterized by a worldwide ecological catastrophe and rapid species turnover. Large-scale devastation of forested environments resulting from the Chicxulub asteroid impact likely influenced the evolutionary trajectories of multiple clades in terrestrial environments, and it has been hypothesized to have biased survivorship of non-arboreal lineages across the K–Pg boundary. Here, we evaluate patterns of substrate preferences across the K–Pg boundary among crown group mammals, a group that underwent rapid diversification following the mass extinction. Using Bayesian, likelihood, and parsimony reconstructions, we identify patterns of mammalian ecological selectivity that are broadly similar to those previously hypothesized for birds. Models based on extant taxa indicate predominant K–Pg survivorship among semi- or non-arboreal taxa, followed by numerous independent transitions to arboreality in the early Cenozoic. However, contrary to the predominant signal, some or all members of total-clade Euarchonta (Primates + Dermoptera + Scandentia) appear to have maintained arboreal habits across the K–Pg boundary, suggesting ecological flexibility during an interval of global habitat instability. We further observe a pronounced shift in character state transitions away from plesiomorphic arboreality associated with the K–Pg transition. Our findings are consistent with the hypothesis that predominantly non-arboreal taxa preferentially survived the end-Cretaceous mass extinction, and emphasize the pivotal influence of the K-Pg transition in shaping the early evolutionary trajectories of extant terrestrial vertebrates.

1. Introduction

The Cenozoic Era is colloquially known as the "Age of Mammals", and the modern world is populated by over 6,000 extant mammalian species exhibiting an extraordinary diversity of forms and ecologies (Nowak 1999; Burgin et al. 2018). Numerous authors have noted that the evolutionary history of extant mammalian biodiversity may have been shaped by the Cretaceous-Paleogene (K–Pg) transition, an interval that is associated with a complex set of mammalian extinctions, radiations, and shifts in species richness (Clemens 2002; Archibald 2011; Wilson et al. 2014; Benevento et al. 2019; Brocklehurst et al. 2021). However, the precise influence of the K–Pg transition on the rate, timing, and nature of mammalian diversification is contentious, and may have varied among major mammalian lineages (Hedges et al. 1996; Springer et al. 2003; Bininda-Emonds et al. 2007; Wible et al. 2007; O'Leary et al. 2013; Halliday et al. 2016; Phillips 2016; Pires et al. 2018; Chen et al. 2019; Grossnickle et al. 2019).

Even in the best-sampled North American localities, a comprehensive, direct assessment of global patterns of mammalian ecological changes across the K–Pg boundary is

precluded by the relatively sparse mammalian fossil record in the latest Cretaceous and earliest Paleogene (Davies et al. 2017), though strong patterns of ecological selectivity are expected in light of high estimated rates of mammalian extinction (Wilson 2013; Grossnickle and Newham 2016; Longrich et al. 2016). Surviving mammalian lineages appear to have undergone rapid morphological diversification from primarily small insectivorous or omnivorous forms, and they colonized a wide range of vacant ecological niches in the aftermath of the mass extinction event (Alroy 1999; Smith et al. 2010; O'Leary et al. 2013; Wilson 2014; Halliday and Goswami 2016a; Grossnickle et al. 2019; Lyson et al. 2019, Shelley et al. 2021). Theoretical studies have predicted that fossorial and semi-aquatic mammals may have had a selective advantage across the K–Pg boundary because their substrate preferences would have shielded them from the severe, short-term effects of the Chicxulub asteroid impact such as a hypothesized heat pulse and associated wildfires (Robertson et al. 2004; DeBey and Wilson 2017). Alongside global fires and longer-term climatic effects, the asteroid impact resulted in forest devastation on a global scale (Tschudy et al. 1984; Vajda et al. 2001; Nichols and Johnson 2008; Field et al. 2018; Lyson et al. 2019; Carvalho et al. 2021) and substantially altered floral communities for centuries (Wilf and Johnson 2004, Carvalho et al. 2021). Recent work on birds suggested that the collapse of global forests drove arboreal Mesozoic avialans to extinction at the K–Pg boundary, with multiple subsequent originations of arboreal habits arising among crown birds once forests had recovered (Field et al. 2018).

Here, we investigate patterns of substrate preference evolution across crown group mammals—another major K–Pg boundary-crossing terrestrial vertebrate clade. First, we assessed the evidence for whether mammals were subject to comparable habitat-related selectivity across the K–Pg boundary. We performed ancestral state reconstructions (ASRs) of substrate preferences on alternative phylogenetic hypotheses for extant mammals (Meredith et al. 2011; Upham et al. 2019). Though not definitive, when interpreted within the context of available fossil evidence we consider the results suggestive of a pattern of predominant K–Pg survivorship among semi-arboreal or non-arboreal mammals, with extant mammalian clades characterized by obligately arboreal ecologies generally arising in the early Cenozoic. Second, we examined the relative clade-wide frequencies of particular evolutionary transitions throughout the evolutionary history of Mammalia using a model-based approach. Our analyses identify an interval early in placental mammal evolutionary history marked by a striking increase in inferred transitions toward non-arboreality. Notably, this interval of apparent clade-wide directional selectivity towards non-arboreality aligns with plausibly K–Pg-associated cladogenesis among crown placentals, although we note that the divergence times of early

placental clades remain contentious. Acknowledging these lingering divergence time uncertainties, we contend that our analyses help illuminate the hidden influence of the K–Pg transition on major ecological patterns early in the evolutionary history of placental mammals.

2. Material and methods

Character State Assignment

All 164 mammalian lineages from the time-scaled phylogenetic hypothesis of Meredith et al. (2011), representing most extant family-level phylogenetic diversity, were assigned an ecological character state of arboreal, semi-arboreal, or non-arboreal (electronic supplementary material). Character states reflect where mammals form nests or otherwise reside. More explicitly, we characterize a "nest" as a construct used for: rearing young, resting, or sleeping (examples include the leaf nests of gorillas or the dreys of squirrels). Alternatively, a mammal may reside in a tree without construction of a nest, where its "residence" is primarily used for sleeping or resting, and may involve rearing young but does not involve any structural modifications to the tree (sloths, for example, often find a leafy area in a tree to sleep in but do not modify the tree or its foliage). An arboreal mammal is therefore one that, in the wild, will virtually always reside or nest in a living tree, be it amongst the branches or in an existing tree cavity. To be classed as semi-arboreal, the mammal in question will often reside or nest in a living tree in the wild but does not do so exclusively. In general, for a semi-arboreal mammal, trees are convenient but not essential, and another substrate (e.g., a rock face) may provide a suitable alternative. All species that fall outside these definitions are classed as non-arboreal, such that the mammal in question does not nest or reside in trees at all, or only does so incidentally in a small number of documented cases. We believe this coding strategy is conservative with respect to mammals that exhibit an obligately arboreal ecology for nesting and residence, and it allows us to discriminate among lineages with obligately arboreal habits from those that occupy trees facultatively or opportunistically.

Alternative phylogenetic frameworks

In order to assess the influence of phylogenetic uncertainty on our ancestral ecological reconstructions, we evaluated them with respect to well-supported phylogenetic hypotheses from Meredith et al. (2011) as well as the node-dated maximum clade credibility consensus tree from Upham et al. (2019) and its associated posterior distribution of tree topologies. Both phylogenetic hypotheses are derived from a supermatrix inference approach, with Upham et al. (2019) using sequences for 31 genes (building on the 26 from Meredith et al. 2011). Meredith et

al. (2011) used a family-level approach to build a time-calibrated tree of 164 mammalian lineages, of which 142 were single species, 16 were congeneric chimaerics, and six were chimaerics above the genus level. Upham et al. (2019) employed a method that separated phylogenetic inference into divergences between major lineages ("backbone") and clades at the species level ("patch") (Mishler 1994; Jetz et al. 2012) to generate a phylogeny uniting ~4,100 species. Our analysis scores the subset of taxa in the Upham et al. (2019) dataset that matched the taxon set from the Meredith et al. (2011) analysis. This yielded two complementary phylogenetic consensus topologies with the same taxon set, on which we estimated character evolution. In the 12 cases where the Upham et al. (2019) dataset did not contain the same species as in Meredith et al. (2011), we replaced the missing species with its closest relative with the same character state (Supporting Information, Table S1). By considering these alternative hypotheses, we specifically assess how robust our inferences are to areas of conflict between the two consensus topologies, such as the monophyly of Euarchonta (Primates + Scandentia + Dermoptera; Upham et al. 2019) and the placement of Scandentia as the sister group to Glires (Rodentia + Lagomorpha; Meredith et al. 2011). Upham et al. (2019) cite posterior probabilities of 0.96 for the monophyly of Euarchonta and 0.78 for Dermoptera + Scandentia. Meredith et al. (2011) found that DNA and amino acid trees agree on the monophyly of Scandentia + Glires but with bootstrap support of <90%.

Model selection

We assessed the relative fit of three alternative time-homogeneous transition models with maximum likelihood in the ape (Paradis et al. 2004) and phytools (Revell 2012) *R* packages (R Core Team 2014) on each consensus tree. Following Field et al. (2018), one model comprised two rates, such that transitions among all three character states (arboreal, semi-arboreal, and non-arboreal) were permitted, but transitions to and from semi-arboreality were allowed a different rate from transitions that bypass this intermediate stage. A second model comprised four rates such that transitions from non-arboreal to arboreal were required to pass through semi-arboreality, with separate forward and reverse rates for each pair of state transitions. These models reflect the presumed biological reality that transitioning from non-arboreality to arboreality or vice versa through an intermediate state likely occurs at a different rate than transitions lacking an intermediate state. We also tested a third maximally parameterized (six-rate) model ("ARD" - all rates different) in which forward and reverse rates were allowed to vary across all states.

Hidden Markov Models (HMMs) have emerged as a powerful tool for assessing the possibility that unobserved rate heterogeneity can have an outsized influence on reconstructing the evolutionary history of discrete characters (Beaulieu et al. 2013; Beaulieu and O'Meara 2016; Boyko and Beaulieu 2021). In comparison to time-homogeneous models, which assume that specified character transition rates do not evolve, HMMs provide an elegant solution for evaluating the hypothesis that the mode of character evolution has evolved throughout a clade's evolutionary history. To assess this possibility in our data, we generated three HMMs using the corHMM *R* package (Beaulieu et al. 2013). Our initial analysis of time-homogeneous models revealed that the six-rate ARD and four-rate intermediate model were preferred (Table 1). Therefore, we elected to compare three HMMs based on those models. The first of these consisted of a model that included two rate classes; one with an ARD model and one with the four-rate model. The second and third HMMs reflected ARD models with two or three rate classes, respectively. In all cases, we assumed symmetric transition rates among rate classes. As time-homogeneous models are a special case of HMMs (reflecting one rate class), we compared all evaluated models with the Akaike Information Criterion (AIC).

Reconstructing the evolution of mammalian arboreality

We performed likelihood-based Ancestral State Reconstructions (ASRs) in *R* (R Core Team 2014). We used the ace() likelihood function in ape (Paradis et al. 2004) and a customized implementation of Bayesian stochastic mapping, described below (Bollback 2006; Revell 2012). We also performed maximum parsimony reconstructions using the ancestral.pars() function in the *R* package phangorn (Schliep 2011).

As part of the VertLife initiative (http://vertlife.org/data/mammals/) Upham et al. (2019) provided a set of 10,000 credible phylogenetic trees sampled from the Bayesian posterior distribution estimated in that study. Therefore, for analyses based on the Upham et al. (2019) consensus tree, we leveraged this resource to account for stochastic uncertainty in branch lengths and tree topology. For each of the time-homogeneous models we evaluated, we performed a Bayesian stochastic character mapping analysis across 1,000 sampled trees from the Upham et al. (2019) posterior distribution, and we estimated 500 stochastic character maps on each. These results were then summarized with respect to the Upham et al. (2019) consensus tree. For analyses directly using the consensus trees, we estimated 5,000 stochastic maps.

To make this task computationally tractable, we generated new *R* code to perform these analyses in parallel across multiple CPUs using the "parallel" (R Core Team 2014), "doSNOW"

(Wallig et al. 2020a), and “doParallel” (Wallig et al. 2020b) *R* libraries. Our approach (see simmap_parallel.R; https://github.com/jakeberv/mammal_arboreality) operates on “phylo” or “multiPhylo” tree objects, accelerating several aspects of this analysis. The wrapper function simmap.parallel(), takes minimally as arguments a tree or set of trees, a discrete character dataset, a time-homogeneous model, and a specified assumption about the distribution of character states at the root (optionally equal or following the FitzJohn et al. (2009) root state prior). Briefly, the function first estimates a Q matrix for each of the trees that are passed to it, using fitMK() (Revell 2012), or alternatively accepts an external Q matrix estimate. Then, depending on the options selected, simmap.parallel() generates stochastic character maps on each of the provided trees using fastSimmap() from the *R* package ratematrix (Caetano and Harmon 2017), the estimated Q matrix for each tree, and the stated root prior. Lastly, a final combined multiSimmap object is generated. This output can be parsed by phytools::describe.simmap() with the argument ref.tree set to the target consensus tree on which to summarize the results. We provide additional code to accelerate aspects of this summation in a modified function describe.simmap.alt(), which can otherwise be very time consuming for large numbers of trees (Eliot Miller, *personal communication*, March 2021).

Investigating clade-wide temporal patterns in character transition rates

In addition to individual node and branch reconstructions, we examined the relative frequencies of particular transition types through time across the two consensus trees as well as the posterior tree distribution from Upham et al. (2019). For example, in a two-rate bidirectional model with two states, forward and reverse transition rates can be time-homogeneous while the total counts of particular transition types across all branches vary through time and depend on the structure of the underlying phylogeny. Revell (2017) outlined an approach for visualizing the history of clade-wide changes in character transitions for a discrete character model under stochastic mapping. This approach first takes a stochastic character mapping simulation and partitions the underlying tree into a specified number of time bins. The average number of character transitions across branches and simulations is calculated within each time bin, and then this value is normalized for patterns of cladogenesis by dividing by the total branch length within a time bin. Revell’s (2017) example provides a pragmatic solution for visualizing the behavior of a discrete character model through time in the context of stochastic character mapping.

Here, we refine this approach to allow examination of temporal patterns in the relative frequencies of each transition type from a given model (see rate_through_time.R;

https://github.com/jakeberv/mammal_arboreality). We generate visualizations for stochastic character mapping under the optimal models for the Meredith et al. (2011) and Upham et al. (2019) consensus topologies, as well as for a sample of 1,000 posterior trees from Upham et al. (2019). These visualizations allow us to further examine the hypothesis that patterns of clade-wide trends in transitions toward and away from arboreality may have been influenced by the K–Pg transition.

3. Results

Node reconstructions

Under the preferred four-rate model (Table 1), stochastic mapping supports a pattern whereby arboreality emerged repeatedly and independently among several different clades following the K–Pg mass extinction. We detect at least 10 instances of post-K–Pg transitions to arboreality under the Meredith et al. (2011) framework (Fig. 1) and 11 cases across the Upham et al. (2019) dataset (Fig. 2). These general patterns hold across both alternative topologies and under parsimony and likelihood optimality criteria (Supporting information, Figs. S1-18).

Bayesian stochastic mapping under the flexible ARD model suggests that state transitions that pass through a semi-arboreal intermediate are detected more frequently than direct-transitions from arboreality to non-arboreality or vice versa (Supporting information, Figs. S6, S9, S12). Additionally, the ARD model detects no direct transitions from non-arboreality to arboreality. By contrast, in the two-rate model, direct transitions from non-arboreality to arboreality are detected at a higher frequency than the reverse, while transitions away from semi-arboreality occur at an intermediate frequency (Supporting information, Figs. S2, S8, S11). We interpret these results to suggest that the transitions inferred under the ARD model are more biologically plausible than those under the two-rate model.

Under both the Meredith et al. (2011) and the Upham et al. (2019) consensus topologies, the preferred four-rate and ARD models reconstructed more nodes near the K–Pg boundary as semi-arboreal than did the two-rate model, especially on the Meredith et al. topology (Supporting information, Figs. S5-6, S15-16). Incorporating a sample of 1,000 tree topologies from the posterior distribution of Upham et al. (2019) made little difference in stochastic mapping reconstructions under the two-rate or ARD models (Supporting information, Figs. S15-18). However, for the optimal four-rate model, consideration of posterior topological uncertainty leads to a marked increase in circum K–Pg nodes being recovered as non-arboreal rather than semi-arboreal (compare Fig. 2 to Supporting information, Fig. S14). We suggest this is a consequence of more pronounced changes in the average estimated Q matrix (inset in Fig.

2) observed for the four-rate model when compared to the two-rate or ARD models, summarized across the posterior tree sample. Although both sets of reconstructions are generally consistent with the hypothesis of K–Pg-associated selectivity against arboreality, it is clear that considering information from the Upham et al. (2019) posterior tree set as opposed to relying solely on simplified consensus topologies impacts the interpretation of our node state reconstructions.

The overall signal we detect is consistent with the hypothesis of predominant survivorship of non-arboreal or semi-arboreal mammals across the K–Pg boundary: few lineages reconstructed as predominantly arboreal are inferred to have survived the K–Pg mass extinction. However, our analyses also highlight two possible exceptions: euarchontans and marsupials. On the Meredith et al. (2011) topology under all models, early members of total-clade Primatomorpha (Primates + Dermoptera) are inferred to have either retained arboreal habits across the K–Pg boundary (Fig. 1; Supporting information, Fig. S4-6) or acquired arboreality shortly thereafter (see below). On the Upham et al. (2019) consensus topology, in which Euarchonta (Primates + Dermoptera + Scandentia) is inferred to be monophyletic, arboreality is reconstructed as having arisen along the euarchontan stem lineage in all models (Supporting information, Figs. S13-16). Considering posterior topological uncertainty also leads to Euarchonta being reconstructed as arboreal at the time of the K–Pg transition, whereas the majority of other lineages are reconstructed as non-arboreal under the four-rate model and semi-arboreal otherwise (Fig. 2; Supporting information, Figs. S17-18). Although not supported by Meredith et al. (2011), a monophyletic Euarchonta has frequently been supported by other phylogenetic analyses (Springer et al. 2003; Springer 2004; O'Leary et al. 2013; Chester et al. 2015, 2017). Under parsimony and two likelihood models (four-rate and ARD), most marsupials are additionally reconstructed as having retained arboreal habits across the K–Pg boundary, or acquired them shortly thereafter (Fig. 1; Supporting information, Figs. S4-6, S13-16). However, this signal is diminished when considering the Upham et al. (2019) distribution of topologies (Fig. 2).

Clade-wide temporal patterns in character transition rates

For both the Meredith et al. (2011) and Upham et al. (2019) consensus topologies, the highest frequency of character transitions detected by the optimal four-rate model falls within the range of divergence time uncertainty for many clades whose originations have been proposed to be associated with the K–Pg boundary (see Discussion). Moreover, the temporal sequence of peaks in the relative frequencies of particular character transition types appears to be consistent

with the hypothesis of selection against obligate arboreality leading up to and through the K–Pg boundary (i.e. transitions away from arboreality, followed by transitions toward arboreality, at least as indicated by analyses on the Upham et al. (2019) consensus topology). These patterns are similar for analyses performed on the Meredith et al. (2011) (Figure 3A) and Upham et al. (2019) (Figure 3B) consensus topologies, as well as the Upham et al. (2019) posterior tree sample (Figure 3C). Tracking fluctuations in the relative frequencies of mammalian ecological transitions approaching the K–Pg boundary (Figure 3), the four-rate model first detects a slight uptick and subsequent reduction in clade-wide transitions from arboreal to semi-arboreal character states, which remains low to the present. This initial pulse is followed by (or is perhaps concurrent with) a large peak in transitions from semi-arboreal to non-arboreal character states, which declines gradually to the present. This peak of character transitions toward non-arboreality appears stronger in the analyses employing the Upham et al. (2019) topologies than in the analyses using the Meredith et al. (2011) consensus topology. Subsequently, a peak in clade-wide transitions from semi-arboreal to arboreal character states is detectable in both analyses, which returns to pre K–Pg levels. Temporal patterns of character state changes from non-arboreal to semi-arboreal appear relatively flat in the Meredith et al. (2011) topology, with a stronger uptick associated with other peaks in the Upham et al. (2019) topologies. When interpreting these results, it should be noted that only one type of character transition can occur at a given time on a given branch on a given stochastic map. Therefore, an apparent increase in one type of character state transition may necessarily be associated with a decline in the frequency of a different type of character state transition.

These patterns emphasize that the most dramatic clade-wide mode changes appear to be associated with the interval encompassing many clade originations hypothesized to be related to the K–Pg transition. These results suggest that the early diversification of placental mammals was associated with clade-wide shifts in the relative rates of character transitions toward and away from particular ecological strategies, and that the sequence of these shifts is consistent with the hypothesis that the transient loss of available arboreal habitats at the K–Pg boundary may have driven those changes. Although the presently wide uncertainty in divergence times precludes a definitive statement, it is important to note that if our documented peaks in evolutionary transitions did occur during the Cretaceous, they could be consistent with the “Early Rise Hypothesis.” In that scenario, an ecological radiation of mammals began prior to the Cretaceous-Palaeogene transition, potentially associated with concomitant diversification events among angiosperms and selected groups of insects (Grossnickle et al. 2019a).

4. Discussion

Inference from the fossil record

Our ancestral state reconstructions consistently support survivorship patterns favoring predominantly non-arboreal or semi-arboreal substrate use across the K–Pg boundary, under likelihood, Bayesian, and parsimony models. This is consistent with previous ASR approaches that recover early mammalian nodes as mostly non-arboreal until just after the K-Pg boundary (Wu et al. 2017). With few exceptions (Lyson et al. 2019), well-preserved mammalian fossils from close to the K–Pg boundary and the first ca. one million years of the extinction's aftermath are exceedingly rare (Williamson 1996; Hartman 2002; Lofgren et al. 2004; Wilson et al. 2014). Most fossils known from this interval are too fragmentary to robustly inform reconstructions of substrate preferences. Indeed, even in cases where strong inferences about the predominant substrate use of a fossil taxon can be drawn, uncertainty regarding parameters such as nesting behaviors is unavoidable. Uncertainty surrounding the phylogenetic position of such fossils presents further challenges with respect to interpreting their implications for early ecological transitions among crown placentals (Halliday et al. 2017). Accepting these limitations, our reconstructions are consistent with the preferential survivorship of non-arboreal mammals across the K–Pg mass extinction. In contrast to evolutionary patterns among crown birds, in which strong selection for non-arboreal ecologies appears to be unambiguously supported by both phylogenetic and fossil evidence (Field et al. 2018, Field et al. 2020a), definitive assessments of selective patterns among K–Pg boundary-crossing mammals will remain elusive in the absence of additional fossil evidence. Until that time, we interpret our results in the context of the currently known circum-K–Pg mammalian fossil record, as well as the more complete records from earlier and later in mammalian evolutionary history.

Based on postcranial morphology, some early (ca.125 Ma) therians including *Eomaia* (Ji et al. 2002), *Ambolestes* (Bi et al. 2018), and *Sinodelphys* (Luo et al. 2003), have been interpreted as arboreal or scansorial, as has the oldest known therian, the ca. 160 Ma *Juramaia* (Luo et al. 2011). Mammalian arboreality may have been common in the Mesozoic, concurrent with increasing mammalian locomotor diversity (Chen and Wilson 2015; Grossnickle et al. 2019). In contrast, later pre-K–Pg lineages for which locomotor reconstructions are possible, such as the metatherian *Asiatherium* (Trofimov and Szalay 1994) and the eutherians *Barunlestes* and *Zalambdalestes* (Kielan-Jaworowska 1978; Chester et al. 2010, 2012) are not interpreted to have been arboreal (Chen and Wilson 2015). Inclusion of Mesozoic fossil taxa in our reconstructions would likely inflate posterior estimates for early arboreality among mammals. However, given our focus on the K–Pg transition and not the ancestral condition of

358 the earliest crown mammals, we elected to restrict our analyses to taxa whose nesting and
359 residence ecology can be scored consistently and systematically.
360 Compared to other major crown mammalian subclades, we infer early arboreal substrate
361 use in Primatomorpha (Meredith et al. 2011) and Euarchonta (Upham et al. 2019), implying
362 either a rapid adoption of arboreality as forests recovered following the K–Pg transition, or
363 retention of at least facultative arboreality across the extinction event. Although relevant fossil
364 data are limited, we can evaluate the primatomorphan and euarchontan fossil record in order to
365 draw inferences about the relative likelihood of these alternative scenarios. The oldest total
366 group primates known from the fossil record (Chester and Sargis 2020), including the stem
367 primates *Purgatorius* and *Torrejonia* and the crown primate *Teilhardina,* date to within
368 approximately 10 million years following the K–Pg transition (Chester et al. 2015, 2019; Morse
369 et al. 2019). These fossils provide insight into ancestral primate habits in the aftermath of the
370 end-Cretaceous mass extinction. From studies of postcranial morphology, *Purgatorius* and other
371 stem primates like *Torrejonia* are reconstructed as having been specialized for arboreal habits
372 (Chester et al. 2015, 2019). As stem primates, this hypothesis is consistent with our inference
373 that primatomorphans (Meredith et al. 2011) or euarchontans (Upham et al. 2019) may have
374 retained a capacity for arboreality through the K–Pg. The inferred arboreal habits of this lineage
375 across the K–Pg boundary is intriguing in light of an apparently strong selective filter against
376 arboreal birds at this same time (Field et al. 2018), as well as theoretical and paleobotanical
377 evidence suggesting forest devastation on a global scale following the Chicxulub asteroid
378 impact (Tschudy et al. 1984; Vajda et al. 2001). Although primatomorphans or euarchontans
379 may have retained arboreal habits in hypothetical forested refugia throughout the K–Pg
380 transition, behavioral flexibility and facultative non-arboreality may also have facilitated the
381 survival of arboreally adapted early primatomorphans across the K–Pg. Though extant colugos
382 are specialized gliders and strict herbivores, extant primates have been hypothesized to be
383 resilient in the face of rapid environmental change on account of their sociality, cognition, and
384 dietary and locomotor flexibility (Morris et al. 2011; Mekonnen et al. 2018), and at least some of
385 these and other traits (e.g., omnivory and small body size in the oldest known stem and crown
386 primates; (Szalay and Delson 1979)) may have contributed to the survival of representatives of
387 the primate total group when facing the devastation of forests at the end-Cretaceous.
388 There is evidence under some of our models that the early evolutionary history of crown
389 marsupials may have also occurred in an arboreal ecological context (Fig. 1; Supporting
390 information, Figs. S4, S6, S13-14, S16, S18). Our ARD model and in some cases the similar
391 four-rate model yield an arboreal reconstruction for the most recent common ancestor of crown

marsupials (Fig. 1; Supporting information, Figs. S6, S14, S16, S18). This inference implies repeated losses of arboreality among marsupials, which would be consistent with the hypothesized retention of plesiomorphic arboreal features in their hands and feet (Bensley 1901; Haines 1958; Szalay 1984). Marsupials suffered some of the greatest diversity loss and longest recovery times in the wake of the K–Pg compared with other boundary-crossing mammalian groups (Pires et al. 2018), and we infer a signal of consistent arboreality among several marsupial lineages near the K–Pg boundary. This is congruent with the earliest known post-K–Pg metatherian skeletons from the early Paleocene of Bolivia, which have been reconstructed as scansorial, with *Mayulestes* inferred to be more specialized for arboreality than *Pucadelphys* (Argot 2003).

Notably, although the fossil record of stem-group bats (Chiroptera) is sparse, the ancestors of crown bats may have been arboreal before they acquired a capacity for powered flight (Gunnell and Simmons 2005; Bishop 2008). However, our results reconstruct much of the chiropteran total-group as predominantly non-arboreal through most of the Paleocene and extending back into the Cretaceous (Fig. 2) (or, in the case of the ARD and four-rate models, potentially semi-arboreal). This is probably a result of the strict application of our character state definitions, where most extant bats were classified as non-arboreal. Many bat species are cave-roosting—thus, they are classified as non-arboreal or semi-arboreal in our analyses, highlighting the fact that our classification of “non-arboreality” does not necessarily imply a predominantly ground-dwelling ecology.

A number of major clades whose extant representatives exhibit arboreality across multiple family-level subclades (e.g., primatomorphans or euarchontans, marsupials, and xenarthrans) may have retained a capacity for arboreal habits across the K-Pg boundary and may have already been adapted to exploit arboreal niches relatively quickly as these habitats recovered. By contrast, arboreal latecomers (e.g., dormice, tree squirrels, bats) independently acquired arboreal habits well into the Cenozoic (Figs. 1, 2). In the case of Xenarthra, the earliest known fossil representatives of this group were likely adapted for fossoriality (Gaudin and Croft 2015), with arboreality in sloths evolving repeatedly and independently throughout the Cenozoic, presumably in response to factors such as diet specialization and predator evasion (Delsuc et al. 2018, 2019). This pattern appears to be reflected in our ASRs: across the majority of our analyses, we infer non-arboreal ecologies for Xenarthra until very shortly after the K–Pg boundary.

As in birds (Mayr 2016; Field et al. 2018), we hypothesize that non-arboreal habits were associated with increased rates of survivorship among mammals across the K–Pg boundary,

consistent with earlier qualitative proposals for enhanced survivorship among burrowing/semi-aquatic mammals (Robertson et al. 2004; DeBey and Wilson 2017). Alongside selection against strict arboreality, many mammalian lineages that passed through the K–Pg mass extinction may have been characterized by reduced body size relative to their pre-extinction antecedents (Lyson et al. 2019); perhaps related to the relationship between body size and total metabolic requirements (McNab 2012; Berv and Field 2018), as well as enhanced survivorship among insectivores and omnivores compared with strict carnivores and herbivores (Sheehan and Hansen 1986; Aberhan et al. 2007). Large-bodied mammals and dietary specialists appear to have been heavily selected against in the immediate wake of the Chicxulub impact (Wilson 2013; Grossnickle and Newham 2016; Lyson et al. 2019), with therians only acquiring their greatest body size range well after the mass extinction when niches previously occupied by large dinosaurs opened (Smith et al. 2010). Multituberculates show a similar increase in the disparity of their body sizes and dental complexity following the K–Pg transition, though their mean body size was apparently unaffected (Wilson et al. 2012; Weaver and Wilson 2020).

Analytical assumptions

The evolutionary scenarios proposed here are conditional on the accuracy of the timescale of the extant mammalian radiation estimated in both the Meredith et al. (2011) and Upham et al. (2019) phylogenies. Divergence times estimated with molecular clock models (Wray 2002; Meredith et al. 2011; Bininda-Emonds et al. 2012) may greatly exceed estimates of clade ages derived from fossil evidence (Wible et al. 2007; Forest 2009; O'Leary et al. 2013), and our understanding of the factors underlying this incongruence is improving (Hillis 1987; Patterson 1987; Novacek 1993; Larson 1998; Springer et al. 2003, 2013; Brochu et al. 2004; Springer 2004; O'Leary et al. 2013; Phillips 2016; Field et al. 2020b). In Xenarthra, divergence time analyses from molecular clock models have yielded estimates for the age of the crown clade exceeding 70 Ma (Bininda-Emonds et al. 2007), whereas the oldest crown group xenarthran fossils are approximately 59 Ma (O'Leary et al. 2013; Wilson Mantilla et al. 2021). Such discrepancies, which span the K–Pg boundary (ca. 66.02 Ma; Clyde et al. 2016), indicate uncertainty regarding the "true" age of important nodes across the mammalian tree of life. This uncertainty is especially relevant to our reconstructions of crown Primatomorpha, for which molecular divergence time analyses frequently estimate a Late Cretaceous origin (Bininda-Emonds et al. 2007; Janečka et al. 2007; Meredith et al. 2011), and likewise for Euarchonta (Janečka et al. 2007; Upham et al. 2019). At present, the oldest known total-clade euarchontan—the arboreal stem primate *Purgatorius*—appears shortly after the K–Pg

boundary, ca. 65.9 MYA (Wilson Mantilla et al. 2021). Thus, direct fossil evidence bearing on whether arboreality was retained across the K–Pg boundary in euarchontans or primatomorphans is lacking. If the "true" node age is younger than the K-Pg boundary, it would imply that arboreality may have emerged post-extinction in Euarchonta or Primatomorpha, rather than arising beforehand and being maintained across the extinction horizon. Lastly, we note that the taxon sample in the present analysis, which is mostly restricted to mammalian family-level clades, could also have introduced some bias into our analysis, though it is difficult to quantify how this might affect our results *a priori* (primarily, we expect transition rates to be under-estimated under the present taxon sampling strategy). Mammalian families that exhibit a range of substrate preferences across extant species-level diversity are necessarily represented in our consensus trees by only a single taxon; 36% of such families were scored as arboreal. Therefore, further exploration of these questions in the context of an expanded taxon sample would provide a fruitful direction for future research.

5. Conclusions

The short-term ecological ramifications of the K–Pg mass extinction are difficult to fully assess from our vantage point 66 million years later, but it is increasingly clear that the evolutionary trajectories of arboreal lineages across the vertebrate tree of life were deeply impacted by this mass extinction event (Vajda et al. 2001; Feng et al. 2017; Field et al. 2018). Direct fossil evidence of mammalian ecological habits from the latest Cretaceous and Paleocene will be needed to further test the patterns of mammalian ecological selectivity inferred here. The Late Cretaceous *Deccanolestes* has been interpreted as arboreal, as have its close relatives (the Paleocene adapisoriculids), providing a compelling example of continuous arboreality among non-euarchontan mammals that survived across the K–Pg boundary (Goswami et al. 2011). Although some Late Cretaceous multituberculates have also been proposed to have been arboreal based on isolated fragmentary humeri (DeBey and Wilson 2017), inferences based on the most complete skeletal material support Late Cretaceous forms as predominantly ground dwelling or fossorial (Kielan-Jaworowska 1989; Kielan-Jaworowska and Gambaryan 1994; Weaver et al. 2021), and some Paleocene taxa as arboreal (Krause and Jenkins 1983), suggesting survival of predominantly non-arboreal multituberculates across the K–Pg with post-extinction transitions to arboreality.

Inferences of mammalian ecological evolution will continue to be refined in light of ongoing improvements in our understanding of mammalian phylogeny, divergence times, and the fossil record (Meredith et al. 2011; O'Leary et al. 2013; Halliday and Goswami 2016b;

Phillips 2016; Grossnickle et al. 2019; Upham et al. 2019). Nevertheless, our new results and simulations are consistent with the hypothesis that the K–Pg transition was a fundamental agent driving ecological shifts in the evolutionary history of Mammalia. The phylogeny of crown group mammals appears to retain the selective signature of end-Cretaceous forest devastation over 66 million years ago, emphasizing the profound degree to which the evolutionary trajectories of extant terrestrial vertebrates were influenced by the K–Pg catastrophe.

ACKNOWLEDGMENTS

We thank Isaac Uyehara for thoughtful discussion and Mark Springer for providing the Newick files used herein. We also thank Jeremy Searle, David Grossnickle, Nathan Upham, and one anonymous reviewer for invaluable comments that improved this manuscript. J.S.B. was supported by a National Science Foundation Graduate Research Fellowship, Doctoral Dissertation Improvement Grant [DGE-1650441, DEB-1700786] and the Michigan Life Sciences Fellows. D.J.F. acknowledges support from the Systematics Association, Isaac Newton Trust Early Career Grant, and UKRI Future Leaders Fellowship [MR/S032177/1].

AUTHOR CONTRIBUTIONS

Jonathan Hughes: Conceptualization (Equal); Data curation (Lead); Formal analysis (Equal); Investigation (Lead); Methodology (Equal); Project administration (Equal); Software (Equal); Validation (Equal); Visualization (Equal); Writing-original draft (Lead); Writing-review & editing (Equal). **Jacob S. Berv:** Conceptualization (Equal); Data curation (Equal); Formal analysis (Lead); Investigation (Equal); Methodology (Lead); Project administration (Equal); Software (Lead); Supervision (Equal); Validation (Equal); Visualization (Lead); Writing-review & editing (Equal). **Stephen G.B. Chester:** Supervision (Equal); Validation (Equal); Writing-review & editing (Equal). **Eric Sargis:** Supervision (Equal); Validation (Equal); Writing-review & editing (Equal). **Daniel J. Field:** Conceptualization (Equal); Funding acquisition (Equal); Investigation (Supporting); Project administration (Equal); Resources (Equal); Supervision (Equal); Writing-review & editing (Equal).

CONFLICT OF INTEREST

The authors declare no conflict of interest.

DATA ACCESSIBILITY

R code will be updated at the author's GitHub repository (https://github.com/jakeberv/mammal_arboreality) and is preserved as a Zenodo archive DOI: 10.5281/zenodo.5338540.

References

Aberhan, M., S. Weidemeyer, W. Kiessling, R. A. Scasso, and F. A. Medina. 2007. Faunal evidence for reduced productivity and uncoordinated recovery in Southern Hemisphere Cretaceous-Paleogene boundary sections. Geology 35:227.

Alroy, J. 1999. The fossil record of North American mammals: evidence for a Paleocene evolutionary radiation. Syst. Biol. 48:107–118.

Archibald, J. D. 2011. Extinction and Radiation: How the Fall of Dinosaurs Led to the Rise of Mammals. John Hopkins University Press, Baltimore, MD.

Argot, C. 2003. Functional-adaptive anatomy of the axial skeleton of some extant marsupials and the paleobiology of the Paleocene marsupials *Mayulestes ferox* and *Pucadelphys andinus*. J. Morphol. 255:279–300.

Beaulieu, J. M., and B. C. O'Meara. 2016. Detecting Hidden Diversification Shifts in Models of Trait-Dependent Speciation and Extinction. Syst. Biol. 65:583–601.

Beaulieu, J. M., B. C. O'Meara, and M. J. Donoghue. 2013. Identifying hidden rate changes in the evolution of a binary morphological character: the evolution of plant habit in campanulid angiosperms. Syst. Biol. 62:725–737.

Benevento, G. L., R. B. J. Benson, and M. Friedman. 2019. Patterns of mammalian jaw ecomorphological disparity during the Mesozoic/Cenozoic transition. P. Roy. Soc. B - B. Sci. 286: 20190347.

Bensley, B. A. 1901. On the question of an arboreal ancestry of the Marsupialia, and the interrelationships of the mammalian subclasses. Am. Nat. 35:117–138.

Berv, J. S., and D. J. Field. 2018. Genomic signature of an avian Lilliput effect across the K-Pg extinction. Syst. Biol. 67:1–13.

Bininda-Emonds, O. R. P., R. M. D. Beck, and R. D. E. MacPhee. 2012. Rocking clocks and clocking rocks: a critical look at divergence time estimation in mammals. Pp. 38–82 *in* R. J. Asher and J. Müller, eds. From Clone to Bone: The Synergy of Morphological and Molecular Tools in Palaeobiology. Cambridge University Press, Cambridge UK.

Bininda-Emonds, O. R. P., M. Cardillo, K. E. Jones, R. D. E. MacPhee, R. M. D. Beck, R.

Grenyer, S. A. Price, R. A. Vos, J. L. Gittleman, and A. Purvis. 2007. The delayed rise of present-day mammals. Nature 446:507–512.

Bishop, K. L. 2008. The evolution of flight in bats: narrowing the field of plausible hypotheses. Q. Rev. Biol. 83:153–169.

Bi, S., X. Zheng, X. Wang, N. E. Cignetti, S. Yang, and J. R. Wible. 2018. An Early Cretaceous eutherian and the placental-marsupial dichotomy. Nature 558:390–395.

Bollback, J. P. 2006. SIMMAP: stochastic character mapping of discrete traits on phylogenies. BMC Bioinformatics 7:88–94.

Boyko, J. D., and J. M. Beaulieu. 2021. Generalized Hidden Markov Models for Phylogenetic Comparative Datasets. Methods Eco. Evol. 12:468–478.

Brochu, C. A., C. D. Sumrall, and J. M. Theodor. 2004. When clocks (and communities) collide: estimating divergence time from molecules and the fossil record. J. Paleontol. 78:1–6.

Brocklehurst, N., E Panciroli, G. L. Benevento, and R. B. J. Benson. 2021. Mammaliaform extinctions as a driver of the morphological radiation of Cenozoic mammals. Curr. Biol. 31(13): 2955–2963.e4.

Burgin, C. J., J. P. Colella, P. L. Kahn, and N. S. Upham. 2018. How many species of mammals are there? J. Mammal. 99:1–14.

Caetano, D. S., and L. J. Harmon. 2017. ratematrix: An R package for studying evolutionary integration among several traits on phylogenetic trees. Methods Ecol. Evol. 8:1920–1927. Wiley.

Carvalho, M. R., C. Jaramillo, F. de la Parra, D. Caballero-Rodríguez, F. Herrera, S. Wing, B. L. Turner, C. D'Apolito, M. Romero-Báez, P. Narváez, C. Martínez, M. Gutierrez, C. Labandeira, G. Bayona, M. Rueda, M. Paez-Reyes, D. Cárdenas, Á. Duque, J. L. Crowley, C. Santos, and D. Silvestro. 2021. Extinction at the end-Cretaceous and the origin of modern Neotropical rainforests. Science 372:63–68.

Chen, M., C. A. E. Strömberg, and G. P. Wilson. 2019. Assembly of modern mammal community structure driven by Late Cretaceous dental evolution, rise of flowering plants, and dinosaur demise. Proc. Natl. Acad. Sci. U.S.A. 116:9931–9940.

Chen, M., and G. P. Wilson. 2015. A multivariate approach to infer locomotor modes in Mesozoic mammals. Paleobiology 41:280–312.

Chester, S. G. B., J. I. Bloch, D. M. Boyer, and W. A. Clemens. 2015. Oldest known euarchontan tarsals and affinities of Paleocene *Purgatorius* to Primates. Proc. Natl. Acad. Sci. U.S.A. 112:1487–1492.

Chester, S. G. B., and E. J. Sargis. 2020. Pan-Primates. Pp. 903–906 *in* K. de Queiroz, P. D.

575 Cantino, and J. A. Gauthier, eds. Phylonyms: A Companion to the PhyloCode. CRC Press,
576 Boca Raton, FL.
577 Chester, S. G. B., E. J. Sargis, F. S. Szalay, J. David Archibald, and A. O. Averianov. 2010.
578 Mammalian Distal Humeri from the Late Cretaceous of Uzbekistan.
579 Chester, S. G. B., E. J. Sargis, F. S. Szalay, J. David Archibald, and A. O. Averianov. 2012.
580 Therian Femora from the Late Cretaceous of Uzbekistan.
581 Chester, S. G. B., T. E. Williamson, J. I. Bloch, M. T. Silcox, and E. J. Sargis. 2017. Oldest
582 skeleton of a plesiadapiform provides additional evidence for an exclusively arboreal
583 radiation of stem primates in the Palaeocene. R. Soc. Open Sci. 4:170329.
584 Chester, S. G. B., T. E. Williamson, M. T. Silcox, J. I. Bloch, and E. J. Sargis. 2019. Skeletal
585 morphology of the early Paleocene plesiadapiform *Torrejonia wilsoni* (Euarchonta,
586 Palaechthonidae). J. Hum. Evol. 128:76–92.
587 Clemens, W. A. 2002. Evolution of the mammalian fauna across the Cretaceous-Tertiary
588 boundary in northeastern Montana and other areas of the Western Interior. *in* J. H.
589 Hartman, K. R. Johnson, and D. J. Nichols, eds. The Hell Creek Formation and the
590 Cretaceous-Tertiary boundary in the northern Great Plains: An Integrated continental
591 record of the end of the Cretaceous. Geological Society of America, Boulder, CO.
592 Davies, T. W., M. A. Bell, A. Goswami, and T. J. D. Halliday. 2017. Completeness of the
593 eutherian mammal fossil record and implications for reconstructing mammal evolution
594 through the Cretaceous/Paleogene mass extinction. Paleobiology. 43(4): 521–536.
595 DeBey, L. B., and G. P. Wilson. 2017. Mammalian distal humerus fossils from eastern Montana,
596 USA with implications for the Cretaceous-Paleogene mass extinction and the adaptive
597 radiation of placentals. Palaeontol. Electron. 20.3.49A:1–92.
598 Delsuc, F., M. Kuch, G. C. Gibb, J. Hughes, P. Szpak, J. Southon, J. Enk, A. T. Duggan, and H.
599 N. Poinar. 2018. Resolving the phylogenetic position of Darwin's extinct ground sloth
600 (*Mylodon darwinii*) using mitogenomic and nuclear exon data. P. R. Soc. B 285:20180214.
601 Delsuc, F., M. Kuch, G. C. Gibb, E. Karpinski, D. Hackenberger, P. Szpak, J. G. Martínez, J. I.
602 Mead, H. G. McDonald, R. D. E. MacPhee, G. Billet, L. Hautier, and H. N. Poinar. 2019.
603 Ancient mitogenomes reveal the evolutionary history and biogeography of sloths. Curr. Biol.
604 29:2031–2042.e6.
605 Feng, Y.-J., D. C. Blackburn, D. Liang, D. M. Hillis, D. B. Wake, D. C. Cannatella, and P. Zhang.
606 2017. Phylogenomics reveals rapid, simultaneous diversification of three major clades of
607 Gondwanan frogs at the Cretaceous–Paleogene boundary. Proc. Natl. Acad. Sci. U.S.A.
608 114:E5864–E5870.

609 Field, D. J., A. Bercovici, J. S. Berv, R. Dunn, D. E. Fastovsky, T. R. Lyson, V. Vajda, and J. A.
610 Gauthier. 2018. Early evolution of modern birds structured by global forest collapse at the
611 end-Cretaceous mass extinction. Curr. Biol. 28:1825–1831.e2.
612 Field, D. J., J. Benito, A. Chen, J. W. M. Jagt, and D. T. Ksepka. 2020a. Late Cretaceous
613 neornithine from Europe illuminates the origins of crown birds. Nature. 579: 397–401.
614 Field, D. J., J. S. Berv, A. Y. Hsian, R. Lanfear, M. J. Landis, and A. Dornburg. 2020b. Timing
615 the extant avian radiation: the rise of modern birds, and the importance of modeling
616 molecular rate variation. Pp. 159–181 *in* M. Pittman and X. Xu, eds. Pennaraptoran
617 theropod dinosaurs: past progress and new frontiers. Bull. Am. Mus. Nat. Hist., New York.
618 FitzJohn, R. G., W. P. Maddison, and S. P. Otto. 2009. Estimating trait-dependent speciation
619 and extinction rates from incompletely resolved phylogenies. Syst. Biol. 58:595–611.
620 Forest, F. 2009. Calibrating the Tree of Life: fossils, molecules and evolutionary timescales.
621 Ann. Bot. 104:789–794.
622 Gaudin, T. J., and D. A. Croft. 2015. Paleogene Xenarthra and the evolution of South American
623 mammals. J. Mammal. 96:622–634.
624 Goswami, A., G. V. R. Prasad, P. Upchurch, D. M. Boyer, E. R. Seiffert, O. Verma, E.
625 Gheerbrant, and J. J. Flynn. 2011. A radiation of arboreal basal eutherian mammals
626 beginning in the Late Cretaceous of India. Proc. Natl. Acad. Sci. U.S.A. 108:16333–16338.
627 Grossnickle, D. M., and E. Newham. 2016. Therian mammals experience an ecomorphological
628 radiation during the Late Cretaceous and selective extinction at the K–Pg boundary. P.
629 Roy. Soc. B - B. Sci. 283:20160256.
630 Grossnickle, D. M., S. M. Smith, and G. P. Wilson. 2019. Untangling the multiple ecological
631 radiations of early mammals. Trends Ecol. Evol. 34:936–949.
632 Gunnell, G. F., and N. B. Simmons. 2005. Fossil evidence and the origin of bats. J. Mammal.
633 Evol. 12:209–246.
634 Haines, R. W. 1958. Arboreal or terrestrial ancestry of placental mammals. Quart. Rev. Biol.
635 33:1–23.
636 Halliday, T. J. D., P. Upchurch, and A. Goswami. 2016. Eutherians experienced elevated
637 evolutionary rates in the immediate aftermath of the Cretaceous–Palaeogene mass
638 extinction. P. Roy. Soc. B - B. Sci. 283: 20153026.
639 Halliday, T. J. D., and A. Goswami. 2016a. Eutherian morphological disparity across the end-
640 Cretaceous mass extinction. Biol. J. Linn. Soc. 118: 152–168.
641 Halliday, T. J. D., and A. Goswami. 2016b. The impact of phylogenetic dating method on
642 interpreting trait evolution: a case study of Cretaceous –Palaeogene eutherian body-size

643 evolution. Biol. Lett. 12: 20160051.
644 Halliday, T. J. D., P. Upchurch, and A. Goswami. 2017. Resolving the relationships of
645 Paleoceneplacental mammals. Biol. Rev. 92: 521–550.
646 Hartman, J. H. 2002. Hell Creek Formation and the early picking of the Cretaceous-Tertiary
647 boundary in the Williston Basin. Pp. 1–7 *in* J. H. Hartman, K. R. Johnson, and D. J. Nichols,
648 eds. The Hell Creek Formation and the Cretaceous-Tertiary boundary in the northern Great
649 Plains: An Integrated continental record of the end of the Cretaceous. Geological Society of
650 America.
651 Hedges, S. B., P. H. Parker, C. G. Sibley, and S. Kumar. 1996. Continental breakup and the
652 ordinal diversification of birds and mammals. Nature 381:226–229.
653 Hillis, D. 1987. Molecular versus morphological approaches to systematics. Annu. Rev. Ecol.
654 Syst. 18:23–42.
655 Janečka, J. E., W. Miller, T. H. Pringle, F. Wiens, A. Zitzmann, K. M. Helgen, M. S. Springer,
656 and W. J. Murphy. 2007. Molecular and genomic data identify the closest living relative of
657 primates. Science 318:792–794.
658 Jetz, W., G. H. Thomas, J. B. Joy, K. Hartmann, and A. O. Mooers. 2012. The global diversity of
659 birds in space and time. Nature 491:444–448.
660 Ji, Q., Z.-X. Luo, C.-X. Yuan, J. R. Wible, J.-P. Zhang, and J. A. Georgi. 2002. The earliest
661 known eutherian mammal. Nature 416:816–822.
662 Kielan-Jaworowska, Z. 1978. Evolution of the therian mammals in the Late Cretaceous of Asia.
663 Part III. Postcranial skeleton in Zalambdalestidae. Palaeontologia Polonica 38:3–41.
664 Kielan-Jaworowska, Z. 1989. Postcranial skeleton of a Cretaceous multituberculate mammal.
665 Acta Palaeontol. Pol. 34:75–85.
666 Kielan-Jaworowska, Z., and P. P. Gambaryan. 1994. Postcranial anatomy and habits of Asian
667 multituberculate mammals. Fossils & Strata 36:1–92.
668 Krause, D. W., and F. A. Jenkins Jr. 1983. The postcranial skeleton of North American
669 multituberculates. Bull. Mus. Comp. Zool. 150:199–246.
670 Larson, A. 1998. The comparison of morphological and molecular data in phylogenetic
671 systematics. Pp. 275–296 *in* R. DeSalle and B. Schierwater, eds. Molecular Approaches to
672 Ecology and Evolution. Birkhäuser, Basel, Switzerland.
673 Lofgren, D. L., J. A. Lillegraven, W. A. Clemens, P. D. Gingerich, and T. E. Williamson. 2004. 3.
674 Paleocene Biochronology: The Puercan Through Clarkforkian Land Mammal Ages. Pp. 43–
675 105 *in* M. O. Woodburne, ed. Late Cretaceous and Cenozoic Mammals of North America.
676 Columbia University Press, New York City, NY.

677 Longrich, N. R., J. Scriberas, and M. A. Wills. 2016. Severe extinction and rapid recovery of
678 mammals across the Cretaceous-Palaeogene boundary, and the effects of rarity on
679 patterns of extinction and recovery. J. Evol. Biol. 29:1495–1512.
680 Luo, Z.-X., Q. Ji, J. R. Wible, and C.-X. Yuan. 2003. An Early Cretaceous tribosphenic mammal
681 and metatherian evolution. Science 302:1934–1940.
682 Luo, Z.-X., C.-X. Yuan, Q.-J. Meng, and Q. Ji. 2011. A Jurassic eutherian mammal and
683 divergence of marsupials and placentals. Nature 476:442–445.
684 Lyson, T. R., I. M. Miller, A. D. Bercovici, K. Weissenburger, A. J. Fuentes, W. C. Clyde, J. W.
685 Hagadorn, M. J. Butrim, K. R. Johnson, R. F. Fleming, R. S. Barclay, S. A. Maccracken, B.
686 Lloyd, G. P. Wilson, D. W. Krause, and S. G. B. Chester. 2019. Exceptional continental
687 record of biotic recovery after the Cretaceous-Paleogene mass extinction. Science
688 366:977–983.
689 Mayr, G. 2016. Avian evolution: the fossil record of birds and its paleobiological significance.
690 Wiley-Blackwell, Hoboken, NJ.
691 McNab, B. K. 2012. Extreme Measures: The Ecological Energetics of Birds and Mammals.
692 University of Chicago Press, Chicago, IL.
693 Mekonnen, A., P. J. Fashing, E. J. Sargis, V. V. Venkataraman, A. Bekele, R. A. Hernandez-
694 Aguilar, E. K. Rueness, and N. C. Stenseth. 2018. Flexibility in positional behavior, strata
695 use, and substrate utilization among Bale monkeys (Chlorocebus djamdjamensis) in
696 response to habitat fragmentation and degradation. Am. J. Primatol. 80:e22760.
697 Meredith, R. W., J. E. Janečka, J. Gatesy, O. A. Ryder, C. A. Fisher, E. C. Teeling, A. Goodbla,
698 E. Eizirik, T. L. L. Simão, T. Stadler, D. L. Rabosky, R. L. Honeycutt, J. J. Flynn, C. M.
699 Ingram, C. Steiner, T. L. Williams, T. J. Robinson, A. Burk-Herrick, M. Westerman, N. A.
700 Ayoub, M. S. Springer, and W. J. Murphy. 2011. Impacts of the Cretaceous Terrestrial
701 Revolution and KPg extinction on mammal diversification. Science 334:521–524.
702 Mishler, B. D. 1994. Cladistic analysis of molecular and morphological data. Am. J. Phys.
703 Anthropol. 94:143–156.
704 Morris, W. F., J. Altmann, D. K. Brockman, M. Cords, L. M. Fedigan, A. E. Pusey, T. S. Stoinski,
705 A. M. Bronikowski, S. C. Alberts, and K. B. Strier. 2011. Low demographic variability in wild
706 primate populations: fitness impacts of variation, covariation, and serial correlation in vital
707 rates. Am. Nat. 177:E14–28.
708 Morse, P. E., S. G. B. Chester, D. M. Boyer, T. Smith, R. Smith, P. Gigase, and J. I. Bloch.
709 2019. New fossils, systematics, and biogeography of the oldest known crown primate
710 *Teilhardina* from the earliest Eocene of Asia, Europe, and North America. J. Hum. Evol.

128:103–131.
Nichols, D. J., and K. R. Johnson. 2008. Plants and the K-T Boundary. Cambridge University Press, Cambridge, UK.
Novacek, M. J. 1993. Mammalian phylogeny: morphology and molecules. Trends Ecol. Evol. 8:339–340.
Nowak, R. M. 1999. Walker's Mammals of the World. 6th ed. John Hopkins University Press, Baltimore, MD.
O'Leary, M. A., J. I. Bloch, J. J. Flynn, T. J. Gaudin, A. Giallombardo, N. P. Giannini, S. L. Goldberg, B. P. Kraatz, Z.-X. Luo, J. Meng, X. Ni, M. J. Novacek, F. A. Perini, Z. S. Randall, G. W. Rougier, E. J. Sargis, M. T. Silcox, N. B. Simmons, M. Spaulding, P. M. Velazco, M. Weksler, J. R. Wible, and A. L. Cirranello. 2013. The placental mammal ancestor and the post-K-Pg radiation of placentals. Science 339:662–667.
Paradis, E., J. Claude, and K. Strimmer. 2004. APE: Analyses of Phylogenetics and Evolution in R language. Bioinformatics 20:289–290.
Patterson, C. 1987. Molecules and Morphology in Evolution: Conflict Or Compromise? Cambridge University Press, Cambridge, UK.
Phillips, M. J. 2016. Geomolecular dating and the origin of placental mammals. Syst. Biol. 65:546–557.
Pires, M. M., B. D. Rankin, D. Silvestro, and T. B. Quental. 2018. Diversification dynamics of mammalian clades during the K-Pg mass extinction. Biol. Lett. 14:20180458.
R Core Team. 2014. R: A language and environment for statistical computing. R Foundation for Statistical Computing, Vienna, Austria.
Revell, L. J. 2012. phytools: an R package for phylogenetic comparative biology (and other things). Methods Evol. Ecol. 3:217–223.
Revell, L. J. 2017. Visualizing the rate of change in a discrete character through time. *Phylogenetic Tools for Comparative Biology*. Accessed 15th Feb 2021. http://blog.phytools.org/2017/11/visualizing-rate-of-change-in-discrete.html
Robertson, D. S., M. C. McKenna, O. B. Toon, S. Hope, and J. A. Lillegraven. 2004. Survival in the first hours of the Cenozoic. Geol. Soc. Am. Bull. 116:760.
Schliep, K. P. 2011. phangorn: phylogenetic analysis in R. Bioinformatics 27:592–593.
Sheehan, P. M., and T. A. Hansen. 1986. Detritus feeding as a buffer to extinction at the end of the Cretaceous. Geology 14:868–870.
Shelley, S. L., S. L. Brusatte, and T. E. Williamson. 2021. Quantitative assessment of tarsal morphology illuminates locomotor behaviour in Palaeocene mammals following the end-

Cretaceous mass extinction. P. Roy. Soc. B - B. Sci. 288:20210393.
Smith, F. A., A. G. Boyer, J. H. Brown, D. P. Costa, T. Dayan, S. K. M. Ernest, A. R. Evans, M. Fortelius, J. L. Gittleman, M. J. Hamilton, L. E. Harding, K. Lintulaakso, S. K. Lyons, C. McCain, J. G. Okie, J. J. Saarinen, R. M. Sibly, P. R. Stephens, J. Theodor, and M. D. Uhen. 2010. The evolution of maximum body size of terrestrial mammals. Science 330:1216–1219.
Springer, M. 2004. Molecules consolidate the placental mammal tree. Trends Ecol. Evol. 19:430–438.
Springer, M. S., R. W. Meredith, E. C. Teeling, and W. J. Murphy. 2013. Technical Comment on "The Placental Mammal Ancestor and the Post-K-Pg Radiation of Placentals." Science 341:613.
Springer, M. S., W. J. Murphy, E. Eizirik, and S. J. O'Brien. 2003. Placental mammal diversification and the Cretaceous-Tertiary boundary. Proc. Natl. Acad. Sci. U.S.A. 100:1056–1061.
Szalay, F. S. 1984. Arboreality: is it homologous in metatherian and eutherian mammals? Evol. Biol. 18:215–258.
Szalay, F. S., and E. Delson. 1979. Evolutionary History of the Primates. Academic, New York, NY.
Trofimov, B. A., and F. S. Szalay. 1994. New Cretaceous marsupial from Mongolia and the early radiation of Metatheria. Proc. Natl. Acad. Sci. U. S. A. 91:12569–12573.
Tschudy, R. H., C. L. Pillmore, C. J. Orth, J. S. Gilmore, and J. D. Knight. 1984. Disruption of the terrestrial plant ecosystem at the Cretaceous-Tertiary boundary, Western interior. Science 225:1030–1032.
Upham, N. S., J. A. Esselstyn, and W. Jetz. 2019. Inferring the mammal tree: Species-level sets of phylogenies for questions in ecology, evolution, and conservation. PLoS Biol. 17:e3000494.
Vajda, V., J. I. Raine, and C. J. Hollis. 2001. Indication of global deforestation at the Cretaceous-Tertiary boundary by New Zealand fern spike. Science 294:1700–1702.
Wallig, M., Microsoft Corporation, and S. Weston. 2020a. doSNOW: Foreach Parallel Adaptor for the "snow" Package.
Wallig, M., Microsoft Corporation, S. Weston, and D. Tenenbaum. 2020b. doParallel: Foreach Parallel Adaptor for the "parallel" Package.
Weaver, L. N., D. J. Varricchio, E. J. Sargis, M. Chen, W. J. Freimuth, and G. P. Wilson Mantilla. 2021. Early mammalian social behaviour revealed by multituberculates from a

779 dinosaur nesting site. Nat Ecol Evol 5:32–37.
780 Weaver, L. N., and G. P. Wilson. 2020. Shape disparity in the blade-like premolars of
781 multituberculate mammals: functional constraints and the evolution of herbivory. J.
782 Mammal. gyaa029:1–19.
783 Wible, J. R., G. W. Rougier, M. J. Novacek, and R. J. Asher. 2007. Cretaceous eutherians and
784 Laurasian origin for placental mammals near the K/T boundary. Nature 447:1003–1006.
785 Wilf, P., and K. R. Johnson. 2004. Land plant extinction at the end of the Cretaceous: a
786 quantitative analysis of the North Dakota megafloral record. Paleobiology 30:347–368.
787 Williamson, T. E. 1996. The Beginning of the Age of Mammals in the San Juan Basin, New
788 Mexico: Biostratigraphy and Evolution of Paleocene Mammals of the Nacimiento
789 Formation: Bulletin 8. New Mexico Museum of Natural History and Science.
790 Wilson, G. P. 2013. Mammals across the K/Pg boundary in northeastern Montana, U.S.A.:
791 dental morphology and body-size patterns reveal extinction selectivity and immigrant-fueled
792 ecospace filling. Paleobiology 39:429–469.
793 Wilson, G. P. 2014. Mammalian extinction, survival, and recovery dynamics across the
794 Cretaceous-Paleogene boundary in northeastern Montana, USA. In: Wilson, G. P., W. A.
795 Clemens, J. R. Horner, and J. H. Hartman. 2014. Through the End of the Cretaceous in the
796 Type Locality of the Hell Creek Formation in Montana and Adjacent Areas. Geological
797 Society of America, Boulder, CO
798 Wilson, G. P., W. A. Clemens, J. R. Horner, and J. H. Hartman. 2014. Through the End of the
799 Cretaceous in the Type Locality of the Hell Creek Formation in Montana and Adjacent
800 Areas. Geological Society of America, Boulder, CO.
801 Wilson, G. P., A. R. Evans, I. J. Corfe, P. D. Smits, M. Fortelius, and J. Jernvall. 2012. Adaptive
802 radiation of multituberculate mammals before the extinction of dinosaurs. Nature 483:457–
803 460.
804 Wilson Mantilla, G. P., S. G. B. Chester, W. A. Clemens, J. R. Moore, C. J. Sprain, B. T.
805 Hovatter, W. S. Mitchell, W. W. Mans, R. Mundil, and P. R. Renne. 2021. Earliest
806 Palaeocene purgatoriids and the initial radiation of stem primates. R. Soc. Open Sci.
807 8:210050.
808 Wray, G. A. 2002. Dating branches on the tree of life using DNA. Genome Biol.
809 3:Reviews0001.1–Reviews0001.7.
810 Wu, J., T. Yonezawa, and H. Kishino. 2017. Rates of Molecular Evolution Suggest Natural
811 History of Life History Traits and a Post-K-Pg Nocturnal Bottleneck of Placentals.

Table 1: Akaike Information Criterion (AIC) scores for all models evaluated on both the Meredith et al. (2011) and Upham et al. (2019) consensus topologies, indicating that the four-rate model is preferred (lowest AIC score, highlighted gray).

Model	Meredith *et al* 2011	Upham *et al* 2019
2 rate	244.93	244.22
4 rate	231.92	234.30
6 rate	235.90	238.67
HRM 4 rate, 2 cat	245.64	246.21
HRM 6 rate, 2 cat	249.64	250.56
HRM 6 rate, 3 cat	268.69	270.37

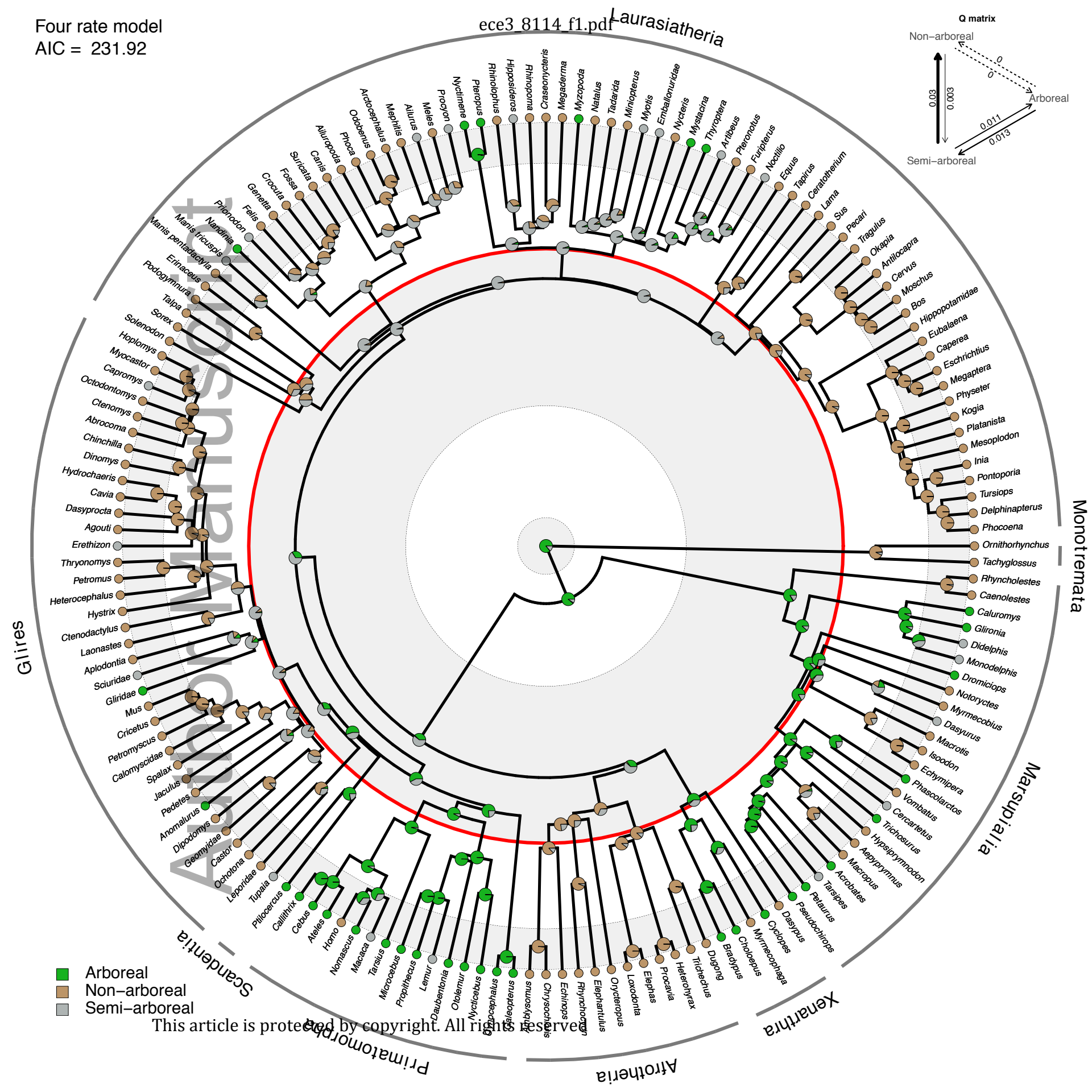

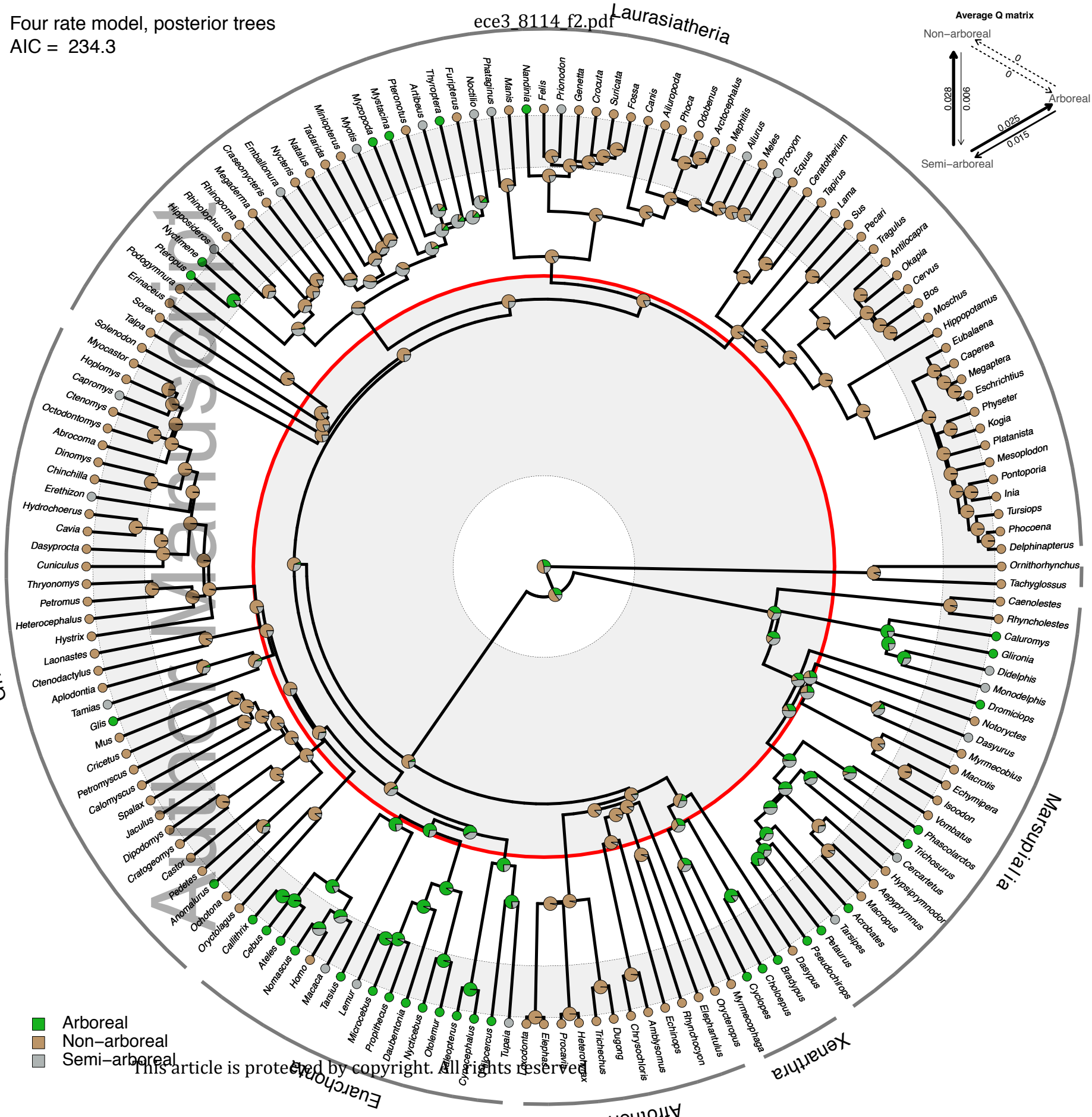
Four rate model, posterior trees
AIC = 234.3
Average Q matrix
Non–arboreal
Arboreal
Semi–arboreal
0.028
0.006
0
0
0.025
0.015
Laurasiatheria
Monotremata
Marsupialia
Xenarthra
Afrotheria
Euarchontoglires
Glires
Manidinia
Felis
Prionodon
Genetta
Crocuta
Suricata
Fossa
Canis
Ailuropoda
Phoca
Odobenus
Arctocephalus
Mephitis
Ailurus
Meles
Procyon
Equus
Ceratotherium
Tapirus
Lama
Sus
Pecari
Tragulus
Antilocapra
Okapia
Cervus
Bos
Moschus
Hippopotamus
Eubalaena
Caperea
Megaptera
Eschrichtius
Physeter
Kogia
Platanista
Mesoplodon
Pontoporia
Inia
Tursiops
Phocoena
Delphinapterus
Ornithorhynchus
Tachyglossus
Caenolestes
Rhyncholestes
Caluromys
Glironia
Didelphis
Monodelphis
Dromiciops
Notoryctes
Dasyurus
Myrmecobius
Macrotis
Echymipera
Isoodon
Vombatus
Phascolarctos
Trichosurus
Cercartetus
Hypsiprymnodon
Aepyprymnus
Macropus
Acrobates
Tarsipes
Petaurus
Pseudochirops
Dasypus
Bradypus
Choloepus
Cyclopes
Myrmecophaga
Orycteropus
Elephantulus
Rhynchocyon
Echinops
Amblysomus
Chrysochloris
Dugong
Trichechus
Heterohyrax
Procavia
Elephas
Loxodonta
Tupaia
Galeopterus
Cynocephalus
Otolemur
Nycticebus
Daubentonia
Propithecus
Microcebus
Lemur
Tarsius
Macaca
Homo
Nomascus
Ateles
Cebus
Callithrix
Oryctolagus
Ochotona
Anomalurus
Pedetes
Castor
Cratogeomys
Dipodomys
Jaculus
Spalax
Calomyscus
Petromyscus
Cricetus
Mus
Glis
Tamias
Aplodontia
Ctenodactylus
Laonastes
Hystrix
Heterocephalus
Petromus
Thryonomys
Cuniculus
Dasyprocta
Cavia
Hydrochoerus
Erethizon
Chinchilla
Dinomys
Abrocoma
Octodontomys
Ctenomys
Capromys
Hoplomys
Myocastor
Solenodon
Talpa
Sorex
Erinaceus
Podogymnura
Pteropus
Nyctimene
Hipposideros
Rhinolophus
Rhinopoma
Megaderma
Craseonycteris
Emballonura
Nycteris
Natalus
Tadarida
Miniopterus
Myotis
Myzopoda
Mystacina
Pteronotus
Artibeus
Thyroptera
Furipterus
Noctilio
Phataginus
Manis
This article is protected by copyright. All rights reserved.
Arboreal
Non–arboreal
Semi–arboreal